Available online at https://link.springer.com/journal/42241
http://www.jhydrodynamics.com
Journal of Hydrodynamics, 2022, 34(6): 1095-1105
https://doi.org/10.1007/s42241-023-0084-1

Dispersion features of pollutants in a compound channel with vegetated floodplains

Yan-fang Zhao[1, 2], Jing-jing Fan[1], Wei-jie Wang[2*], Han-qing Zhao[3, 4], Fei Dong[2], Zhen Han[2], Shi-yan Wang[2]
1. *School of Water Conservancy and Hydroelectric Power, Hebei University of Engineering, Handan 056038, China*
2. *State Key Laboratory of Simulation and Regulation of Water Cycle in River Basin, China Institute of Water Resources and Hydropower Research, Beijing 100038, China*
3. *China Three Gorges Corporation, Wuhan 430010, China*
4. *National Engineering Research Center of Water Resources Efficient Utilization and Engineering Safety, Nanjing 210024, China*

(Received July 11, 2022, Revised September 28, 2022, Accepted September 29, 2022, Published online January 4, 2023)

Abstract: The planting of the vegetation on the floodplain helps the ecological restoration, which is the main form of the river's ecological corridor. Therefore, the current research of the river dynamics focuses on the water movement under a compound channel with the vegetated floodplains. Two simulated vegetation species are selected in this paper for the flume simulation experiments of the floodplain vegetation, and the compound channel is divided into three subregions in the transverse direction. The Navier-Stokes equation and the eddy viscosity theory are applied to obtain the transverse distribution of the depth-averaged velocity and the results agree well with the experimental data. This paper proposes a new method based on the analytical solution of the flow velocity distribution to calculate the average flow velocity in each section. Calculation results can effectively simulate the average flow velocity of the measured sections. The description of the pollutant transport processes in a moving stream requires a refined determination of the dispersion coefficients in the compound channel. The process of the pollutant concentrations in each zone and the reasons for their occurrence are elucidated on the basis of the experimental results. Simultaneously, the measured values of the longitudinal dispersion coefficients are obtained by the "routing procedure," and a two-zone model of the pollutant dispersion is constructed on the basis of the hydrodynamic study. The prediction method for the longitudinal dispersion coefficients is also presented. Applying the predicted and measured section average flow velocities to the two-zone model to predict the longitudinal dispersion coefficient, and the average relative errors are only 4.17%, 7.15%, respectively. This result indicates that the two-zone model can effectively predict the longitudinal dispersion coefficients. The calculation methods for the longitudinal dispersion coefficients from–various studies are compared. The results reveal that the predicted values of these calculation methods are all larger than the measured values, indicating that the vegetation has a considerable influence on the dispersion process. This study comprehensively shows the dispersion features of the pollutants and provides a theoretical basis for the planning and the design of the vegetated ecological corridors.

Key words: Compound channel, floodplain vegetation, velocity distribution, pollutant transport, dispersion coefficient

Introduction

Natural rivers are usually in the form of compound channels, dominated by the main channels and the floodplains, and the vegetation extensively grows on the floodplain and the side slopes of the compound channels. The vegetation changes the flow velocity, promotes the sediment deposition, and increases the resistance of the river bed[1], thus affecting the flood discharge. Moreover, the vegetation can degrade the pollutants, improve the self-purification capability of the water bodies, and provide habitats for aquatic organisms, thereby protecting the biodiversity[2]. The river ecological protection based on planting vegetation has been increasingly and extensively used in recent years. Therefore, the research of the transport characteristics of the pollutants in the compound channel with the vegetated floodplain can provide a theoretical basis for the protection and the construc-

Project supported by the National Key Research and Development Program of China (Grant No. 2019YFD1100205), the National Natural Science Foundation of China (Grant Nos. 51809286, 52209083, 51809288, 41501204 and U1802241).
Biography: Yan-fang Zhao (1996-), Male, Master,
E-mail: zhaoyf130012@163.com
Corresponding author: Wei-jie Wang,
E-mail: wjwang@whu.edu.cn

tion of the river ecology.

Some progress has been made in recent years on the researches of the hydrodynamics of the vegetation channels. Wang et al.[3] conducted flume experiments using rigid cylinders with different densities and found that the coefficient of drag (C_d) is in a distribution close to a parabolic shape in the flow direction x. The higher the vegetation density the more significant is the drag effect. Therefore, the volume resistance equation was proposed. Sun and Shiono[4] established a formula for the resistance coefficient of a vegetated compound channel by using the vegetation density and water flow parameters. Huai et al.[5] investigated the turbulent structure of the submerged flexible vegetation through the flume experiments and it was concluded that the ejection and sweep events had a remarkably effect on the Reynolds stress near the top of the vegetation. Liu et al.[6] divided the longitudinal cross-section into two regions and proposed an exponential decay-based model to predict the velocity distribution for the emergent vegetation. Li et al.[7] studied the effect of the submerged flexible vegetation on the flow structure (the flow velocity, the Reynolds stress, the turbulence intensity, and the Manning's coefficient) in a compound flume and developed the corresponding empirical equations for the flow velocity. Fernandes et al.[8] divided the vegetated compound channel into four zones and obtained the cross-sectional velocity distribution of each zone by studying its secondary flow coefficient. Wang et al.[9] investigated the vegetation of variable frontal widths in the vertical direction and established a flow velocity distribution formula based on the vegetation shape function.

Water flow and associated mass transport are important research contents of environmental hydraulics[10]. The presence of vegetation changes the water flow structure, which has a certain impact on the transport of pollutants. Therefore, a considerable amount of researches was focused on the discrete processes in rivers. Murphy et al.[11] divided the river channel into the vegetated and non-vegetated zones and applied the N-zone model of Chickwendu to solve for the longitudinal dispersion coefficients. Similarly, Huai et al.[12] also adopted a partition model and extended it to a three-zone model. They examined the longitudinal dispersion coefficients and verified the accuracy of the aforementioned model. Liu et al.[13] combined the proposed four-zone model with a random displacement model to investigate the longitudinal dispersion coefficients. Sonnenwald et al.[14] developed a simple dimensionless model based on the flow velocity and the vegetation diameter spacing to predict the longitudinal dispersion coefficients of the low-density emergent vegetation.

Experiments are conducted in this paper using the simulated dwarf grass and sedge in a compound channel. On the basis of solving the flow velocity distribution, the dispersion coefficients are calculated and validated using the N-zone model, and the longitudinal dispersion coefficient calculation formulas proposed by different scholarscompared to provide a theoretical method for accurately describing the pollutant transport process.

1. Theory and method

1.1 *Distribution of velocity in compound channels*

In the uniform flow state, the depth-averaged Navier-Stokes equation for a compound channel without vegetation can be expressed as[15]

$$\rho g H S_0 - \frac{1}{8}\rho f U^2 \sqrt{1+\frac{1}{s^2}} + \frac{\partial}{\partial y}\left[\rho \zeta H^2 \left(\frac{f}{8}\right)^{1/2} U \frac{\partial U}{\partial y}\right] = 0 \tag{1}$$

where ρ is the density of the water, g is the gravitational acceleration, S_0 is the bed slope, x, y and z are the directions of the water flow (longitudinal), the river width (transverse) and the water depth (vertical), respectively, U is the depth-average velocity, H is the water depth, s is the slope of the side slope, f is the Darcy-Weisbach friction coefficient and ζ is the eddy viscosity coefficient.

The Darcy-Weisbach coefficient from the friction and eddy-viscosity theory is determined as follows[16]:

$$f = \frac{8\tau_b}{\rho U^2}, \quad \overline{\tau_{xy}} = \rho \xi_{xy} \frac{\partial U}{\partial y},$$

$$\xi_{xy} = \zeta H U_* = \zeta H \left(\frac{f}{8}\right)^{1/2} U \tag{2}$$

where τ_b is the bed shear stress, $\overline{\tau_{xy}}$ is the depth-averaged transverse shear stress, ξ_{xy} is the eddy viscosity and U_* is the shear velocity.

For a compound channel with the emergent or submerged vegetation on the floodplain, the vegetation drag force per unit water body can be expressed as follows: $F_v = 1/2\rho\chi C_d \lambda (U')^2$, where C_d is the drag coe□cient, $\lambda = mD$ is the vegetation coefficient, m is the vegetation density (plants/m^2), D is the vegetation diameter, χ is the vegetation shape coefficient and U' is the time-averaged velo-

city in the x-direction. F_v is integrated along the vegetation height H_v to obtain

$$\int_0^{H_v} F_v \mathrm{d}z = \frac{1}{2}\rho\chi C_d \lambda H_v U_v^2 \tag{3}$$

where U_v is the average flow velocity inside the vegetation.

Based on the force balance, substituting Eq. (3) into Eq. (1) yields the following

$$\rho g H S_0 - \rho\frac{1}{8} f U^2 \sqrt{1+\frac{1}{s^2}} + \frac{\partial}{\partial y}\left[\rho\zeta H^2 \left(\frac{f}{8}\right)^{1/2} U\frac{\partial U}{\partial y}\right] - \frac{1}{2}\rho\chi C_d \lambda H_v U_v^2 = 0 \tag{4}$$

For the floodplain with the submerged vegetation, Stone and Shen[17] proposed the vegetation submergence coefficient h^* to characterize the relationship between U, U_v: $U_v/U = (h^* k_v)^{0.5}$, where $k_v = [(1-Dm^{0.5})/(1-h^* Dm^{0.5})^2$, $h^* = 1$ means the emergent vegetation, and $h^* < 1$ means the submerged vegetation.

The existence of the vegetation will hinder the water flow movement. Therefore, the void coefficient (μ) is introduced to represent the water blocking effect of the vegetation

$$\mu = \frac{V_{\text{column}} - V_{\text{vegetation}}}{V_{\text{column}}} = 1 - m\frac{\pi}{4}D^2 h^* \tag{5}$$

where V_{column} is the volume of unit water column, $V_{\text{vegetation}}$ is the volume of the vegetation in unit water column.

Therefore, under the action of the emergent or submerged vegetation, the depth-averaged momentum equation can be written as

$$\mu\rho g H S_0 - \frac{1}{8}\mu\rho f U^2 \sqrt{1+\frac{1}{s^2}} + \mu\frac{\partial}{\partial y}\left[\rho\zeta H^2 \left(\frac{f}{8}\right)^{1/2} U\frac{\partial U}{\partial y}\right] - \frac{1}{2}\rho\chi C_d \lambda H_v U_v^2 = 0 \tag{6}$$

The entire compound channel is then divided into the following zones: A main channel zone, a side slope zone, and a floodplain zone (correspondingly referred to as the zones 1, 2 and 3, respectively). For the non-vegetated main channel and the side slope zones we have $m = 0$, $\mu = 1$. Solve equation (6):

For the main channel zone, the analytical solution of the governing equation is

$$U_1 = (A_1 \mathrm{e}^{r_1 y} + C_1 \mathrm{e}^{-r_1 y} + k_1)^{1/2} \tag{7}$$

where

$$r_1 = \sqrt{\frac{f}{4\zeta H^2 (f/8)^{1/2}}} \tag{8}$$

$$k_1 = \frac{8 g S_0 H}{f} \tag{9}$$

For the linear side slope zone, the analytical solution of the governing equations is

$$U_2 = (A_2 Y^{\alpha_1} + C_2 Y^{-\alpha_1 - 1} + \omega Y)^{1/2} \tag{10}$$

where

$$\alpha_1 = -\frac{1}{2} + \frac{1}{2}\left(1 + \frac{s\sqrt{1+s^2}}{\zeta}\sqrt{8f}\right) \tag{11}$$

$$\omega = \frac{g S_0}{(\sqrt{1+s^2}/s)(f/8) - (\zeta/s^2)\sqrt{f/8}} \tag{12}$$

Y is the water depth function of the side slope zone: $Y = H - (y-b)/s$.

For the floodplain zone with vegetation, the analytical solution of the governing equation is

$$U_3 = (A_3 \mathrm{e}^{r_3 y} + C_3 \mathrm{e}^{-r_3 y} + k_3)^{1/2} \tag{13}$$

where

$$r_3 = \sqrt{\frac{f/8 + (1/2\mu) C_d \lambda k_v (h^*)^2 H}{(1/2)\zeta H^2 (f/8)^{1/2}}} \tag{14}$$

$$k_3 = \frac{g S_0 H}{f/8 + (1/2\mu) C_d \lambda k_v (h^*)^2 H} \tag{15}$$

the value of C_d is calculated using the equation of Schlichting and Gersten[18]. The value of the vegetation shape coefficient is taken as 1. A_1, C_1, A_2,

C_2, A_3 and C_3 are all constants.

Equations (7), (10) and (13) each have two unknown constants. Thus, setting the boundary conditions is necessary to obtain the analytical solution.

(1) Near the walls of the main channel and the floodplain, the flow velocity $U = 0$.

(2) The flow velocity is continuous at the cross-section connection, that is, $U_i = U_{i+1}$.

(3) The velocity gradient is continuous at the cross-section connection, that is, $\partial U_i / \partial y = \partial U_{i+1} / \partial y$.

For the dimensionless eddy viscosity coefficient ζ, Pasche and Rouvé[19] suggested that ζ_1 can be taken as 0.067 in the main channel zone and ζ_2 as 0.134 in the side slope zone, in the vegetated floodplain zone, $\zeta_3 / \zeta_1 = (2D_r)^{-4}$, where D_r is the relative water depth.

The friction coefficient f is derived from the hydraulic formula[16]: $J = fU^2 gR / 8$, $U = n^{-1} R^{2/3} J^{1/2}$. Thus

$$f = \frac{8gn^2}{R^{1/3}} \tag{16}$$

where R is the hydraulic radius, J is the hydraulic gradient and n is the Manning's coefficient.

Based on the analytical solution of the flow velocity distribution in different zones (the main channel, the side slope, and the floodplain), the average flow velocity of the section in different zones is deduced as follows: $U_d = (y_2 - y_1)^{-1} \int_{y_1}^{y_2} U \mathrm{d}y$. The analytical solution of the flow distribution is complicated, and determining its integral form is difficult. Thus, a new method is proposed herein for the calculation of the average flow velocity at the section.

This paper proposes to use $U_d^2 = (y_2 - y_1)^{-1} \int_{y_1}^{y_2} U^2 \mathrm{d}y$ as a method to calculate the average flow velocity of the section to simplify the integral form of the analytical solution of the flow velocity distribution.

In the main channel zone

$$U_{1d}^2 = \frac{1}{y_{12} - y_{11}} \int_{y_{11}}^{y_{12}} U_1^2 \mathrm{d}y = \frac{1}{y_{12} - y_{11}} \cdot \left(\frac{A_1 \mathrm{e}^{r_1 y}}{r_1} - \frac{C_1 \mathrm{e}^{-r_1 y}}{r_1} + k_1 y + M_1 \Big|_{y_{11}}^{y_{12}} \right) \tag{17}$$

In the side slope zone

$$U_{2d}^2 = \frac{1}{y_{22} - y_{21}} \int_{y_{21}}^{y_{22}} U_2^2 \mathrm{d}y = \frac{1}{y_{22} - y_{21}} \cdot \left(\frac{A_2 Y^{\alpha_1}}{1 + \alpha_1} - \frac{C_2 Y^{-\alpha_1}}{\alpha_1} + \frac{\omega Y^2}{2} + M_2 \Big|_{y_{21}}^{y_{22}} \right) \tag{18}$$

In the floodplain zone

$$U_{3d}^2 = \frac{1}{y_{32} - y_{31}} \int_{y_{31}}^{y_{32}} U_3^2 \mathrm{d}y = \frac{1}{y_{32} - y_{31}} \cdot \left(\frac{A_3 \mathrm{e}^{r_3 y}}{r_3} - \frac{C_3 \mathrm{e}^{-r_3 y}}{r_3} + k_3 y + M_3 \Big|_{y_{31}}^{y_{32}} \right) \tag{19}$$

where U_{1d}, U_{2d} and U_{3d} are the section average flow velocities for different zones, M_1, M_2 and M_3 are the integration constants. y_{11}, y_{12} are the endpoint locations for the main channel zone, y_{21}, y_{22} are the endpoint locations for the side slope zone, y_{31}, y_{32} are the endpoint locations for the floodplain zone.

The accuracy of the model is verified by comparing the predicted and measured values, as comprehensively discussed in Section 3.1.

1.2 *Dispersion coefficient theory and methods*

The longitudinal dispersion coefficient reflects the longitudinal mixing characteristics of the river, and it is mainly influenced by various factors, such as the flow conditions, the cross-section characteristics, and the channel shape. The theory of the shear dispersion effects was firstly proposed by Taylor in 1954. Fischer concluded that the longitudinal dispersion coefficient of the natural rivers is mainly due to the uneven distribution of the longitudinal flow velocities in the transverse direction, Thus, an expression for the longitudinal dispersion coefficient of rivers was given.

$$K = -\frac{1}{A} \int_0^B u''(y) h(y) \int_0^y \frac{1}{M_y(y) h(y)} \int_0^y h(y) u''(y) \mathrm{d}y \mathrm{d}y \mathrm{d}y \tag{20}$$

where A is the river section area, B is the river width, $h(y)$ is the water depth, U_b is the average flow velocity at the section, $M_y(y)$ is the transverse mixing coefficient and $u''(y)$ is the deviation from the average flow velocity at the section.

Various empirical formulas were proposed for

the lateral distribution of the longitudinal flow velocity of the river to calculate the dispersion coefficient through Eq. (20), However, obtaining the flow velocity distribution in the actual natural rivers is difficult. Therefore, various empirical formulas were proposed for dispersion coefficients, and the most commonly used empirical formulas are the ones for longitudinal dispersion coefficients established by Fischer[20], Deng[21], Zeng and Huai[22] and Wang and Huai[23] (Table 1).

Table 1 Empirical formulas for longitudinal dispersion coefficient

Scholar	Empirical formula
Fischer[20]	$K=0.011\left(\frac{U_b}{u_*}\right)^2\left(\frac{B}{H}\right)^2 Hu_*$
Deng[21]	$K=\frac{0.043}{8e(y)_0}\left(\frac{U_b}{u_*}\right)^2\left(\frac{B}{H}\right)^2 Hu_*$
Zeng and Huai[22]	$K=5.4\left(\frac{U_b}{u_*}\right)^{0.13}\left(\frac{B}{H}\right)^{0.7} HU_b$
Wang and Huai[23]	$K=0.0798\left(\frac{U_b}{u_*}\right)^2\left(\frac{B}{H}\right)^{0.6239} Hu_*$

Note: H is the water depth, u_* is the friction velocity, B is the channel width, U_b is the section mean flow velocity and $e(y)_0$ is the transverse diffusion coefficient: $e(y)_0 = 0.145+1/3\,520(U_b/u_*)(B/H)^{1.38}$.

In a two-dimensional open channel partially covered with vegetation, Boxall and Guymer[24] calculated the longitudinal dispersion coefficient by dividing the flow into N sub-zones in the transverse direction.

$$K=\sum_{i=1}^{N-1}(a_1+a_2+\cdots+a_i)^2[1-(a_1+a_2+\cdots+a_i)]^2\cdot$$

$$[V_{1,j}-V_{(i+1),N}]^2/b_{i(i+1)}+\sum_{i=1}^{N}a_iK_i \tag{21}$$

In our experiments, the flume is partially vegetated; therefore, the flume is divided into vegetated and non-vegetated zones, that is, $N=2$. Hence, Eq. (21) can be written as

$$K=\frac{(B_{nv}/B)^2(B_v/B)^2(V_1-V_2)^2}{b_{1,2}}+\frac{B_{nv}}{B}K_1+\frac{B_v}{B}K_2 \tag{22}$$

where B_{nv} is the width of the non-vegetated zone, B_v is the width of the vegetated zone and B is the width of the flume. V_1 and V_2 are the average section flow velocities in the non-vegetated and vegetated zones, respectively, herein, the average section flow velocities calculated by Equations (17), (18) and (19) are used. K_1 is the longitudinal dispersion coefficient for the non-vegetated zones, which satisfies the variation pattern of the longitudinal dispersion coefficient in the non-vegetated channels, and the equation proposed by Wang and Huai[23] is used herein as follows

$$K_1=0.0798\left(\frac{U_b}{u_*}\right)^2\left(\frac{B}{H}\right)^{0.6239}Hu_* \tag{23}$$

where K_2 is the longitudinal dispersion coefficient of the vegetated zone. In the interior of the vegetated zone, the transverse distribution of the longitudinal flow velocities is uniform (Fig. 3), thus, $u''(y)=0$, $K_2\approx 0$. $b_{1,2}$ are transverse mixing coefficients, which are defined by Murphy et al.[11] as the time scale at which a pollutant crosses a vegetated zone in the transverse direction.

$$b_{1,2}^{-1}\approx T\approx\frac{(B_v-\delta_I)^2}{E_y}+\frac{\delta_I}{k} \tag{24}$$

where T is the time scale, δ_I is the width of the shear layer intrusion into the vegetation layer. According to the theory of White and Nepf[25]: $\delta_I\approx\max(0.5C_d^{-1}a^{-1},1.8d)$, where d is the equivalent diameter of the vegetation.

White and Nepf[25] considered the following factors: the exchange coefficient $k=\beta\delta_o 0.032\bar{U}/\theta$, where $\beta=0.3\pm0.04$ is the exchange rate parameter, $\bar{U}=(U_1+U_2)/2$ is the arithmetic mean of the flow velocity in the non-vegetated zone and the flow velocity in the vegetated zone and θ is the momentum thickness. White and Nepf[25] also considered the following factors: $\delta_o/\theta=3.3\pm0.04$. Nepf[26] proposed a transverse diffusion coefficient $E_y=\alpha'(C_dad)^{1/3}V_2d$, where the scale coefficient $\alpha'=0.8$ [27], $a=md$ is the projected area of vegetation per unit height along the flow direction and m is the number of vegetation per unit bed area.

1.3 *Calculation method of measured value of dispersion coefficient*

The measured value of the dispersion coefficient is calculated in accordance with the "routing procedure" proposed by Fischer[28]. The basic idea is to

consider the concentration process $C_2(x_2,t)$ at the downstream section as the result of the diffusion of the time-continuous source $C_1(x_1,t)$ from the upstream section according to the concentration process of the upstream and downstream sections. This approach establishes the relationship between the upstream and downstream concentrations and then can be used to obtain the value of the dispersion coefficient K from the equation below.

$$C_2(x_2,t)=\int_{-\infty}^{\infty}\frac{C_1(x_1,\tau)}{\sqrt{4\pi K(t_2-t_1)}}\cdot \exp\left\{\frac{-[x_2-x_1-U(t-\tau)]^2}{4K(t_2-t_1)}\right\}U\mathrm{d}\tau \tag{25}$$

where τ is the integration variable, t_i is the average time when the pollutants pass through the measuring point x_i and U is the flow velocity of the pollutants.

2. Experiment

The experiment is conducted in a rectangular flume at the Institute of Water Ecology and Environment, China Institute of Water Resources and Hydropower Research, with the experiment flume of length× width×depth =10.0 m×1.0 m×1.0 m. The bottom of the flume is laid with the PVC formwork, and the walls are made of glass. The flume is divided transversely into the following three zones: The main channel, the side slope, and the floodplain, of which the width of the main channel zone is 0.4 m, the height and the width of the side slope zone are both 0.2 m, and the height and the width of the floodplain zone are 0.2 m, 0.4 m, respectively. The specific flume parameters are shown in Fig. 1. The water flume is a recirculating flume, and the water level in the flume is kept to the requirements of each working condition by controlling the upstream valve and the downstream tailgate to maintain constant and uniform flow conditions. The simulated vegetation of the short grass and the sedge is used in this experiment as the research object (Fig. 1). The flow velocity is measured using acoustic Doppler velocimetry (ADV), which is based on the Doppler principle and uses the telemetry to measure a sampling point at a certain distance from the probe. The concentration process of the rhodamine reagents is measured using a multiparameter water quality meter (YSI), which has the advantage of high automation and accuracy, and the frequency of the measurement can be set in accordance with the working conditions.

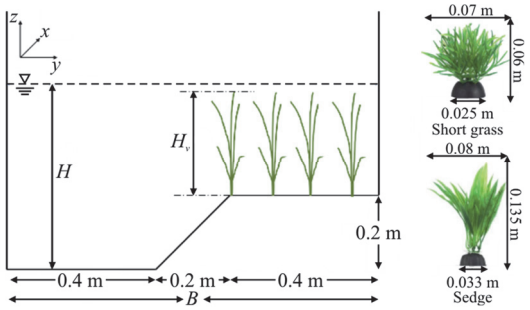

Fig. 1 (Color online) Schematic diagram of a compound channel section

In this experiment, the vegetation is laid on the bottom of the riverbed in a parallel manner. The transverse interval in the vegetation is 0.1 m, the longitudinal interval is 0.075 m, and the length of the covered riverbed is 8 m. The fully developed area of the water flow is as follows: $X_B=\min\{3.5B, 7h\}$ [29-30], where B is the flume width, h is the submerged vegetation height. In this experiment, the vegetation height is small; and in view of the pipeline inflow at the front of the flume and the vegetation blocking effect, the water flow can be fully developed when $X_B=6.6$ m. Therefore, the measurement section of the flow velocity is selected herein, and the sampling points for the pollutant concentration measurement are also located in this fully developed area. The ADV used in this experiment is a lateral probe. The sampling point is located 0.05 m in front of the probe, the sampling frequency is 200 Hz, and the sampling time is 2 min. Meanwhile, the vertical distance between the sampling points is 0.010 m-0.015 m, and each sampling point is a total of 24 000 data. The YSI is used to measure the concentration process of the rhodamine tracer. At the section 0.5 m away from the entrance of the water flume, the injector is used to put the rhodamine solution tracer ($C_0=10$ g / L) at the position of $z=0.5H_w$. The point is located 3.5 m downstream the injection section, and the second measurement point is located 6.5 m downstream the injection section. Simultaneously, the section is divided into three zones, and three sets of parallel experiments are performed in each section. This experiment is conducted on the basis of different water depths and vegetation species, and the specific working measurement lines and experimental parameters are shown in Fig. 2, Table 2, respectively.

3. Results and discussions

3.1 *Flow velocity distribution results*

Figure 3 shows the transverse distribution of the

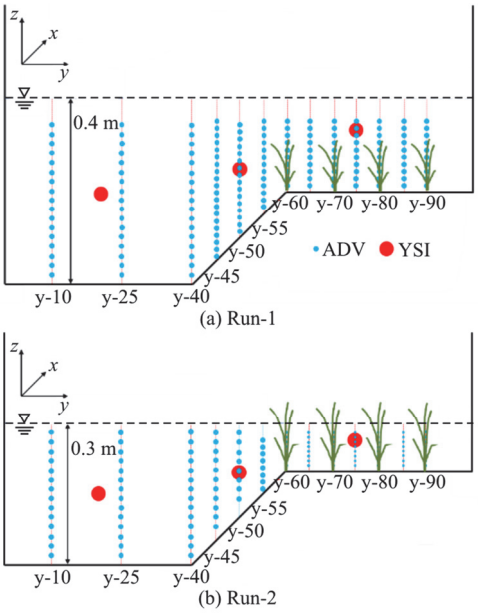

Fig. 2 (Color online) Schematic diagram of a compound channel lateral

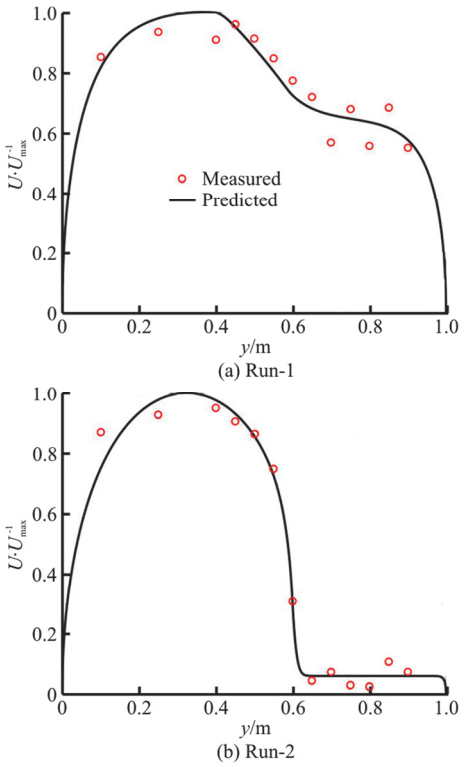

Fig. 3 (Color online) Analytical solution of the flow velocity distribution

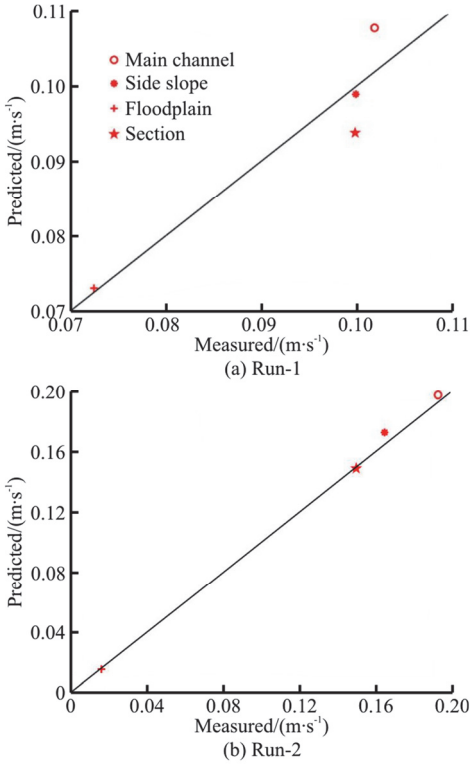

Fig. 4 (Color online) Comparison of the average flow velocity of the section

depth-averaged flow velocity in the compound channel under different working conditions, and the results indicate that the model predictions are in good agreement with the experimental measurements. This figure reveals that the transversal distribution of the longitudinal flow velocities is similar for the cases Run-1, Run-2. The flow velocity in the case Run-2 is higher than that in the case Run-1 at the same position in the main channel and side slope zones because of the smaller water depth and sectional area in the case Run-2 than in the case Run-1. Meanwhile, in the case Run-1, the same flow rate is adopted as in the case Run-2, resulting in a high flow velocity in the case Run-1. In the floodplain zone, the flow velocity is mainly influenced by the vegetation and is smaller in the case Run-2 than in the case Run-1 at the same position. This phenomenon is due to the non-submerged vegetation in the case Run-2 and its considerable blocking effect on the flow, resulting in a low flow velocity.

Figure 4 shows a comparison of the average sectional flow velocities in different zones in a compound channel under different working conditions.

Table 2 Parameter table

Run	H_v /m	D_{min}	D_{max}	Q /(m³·s^{-1})	H /m	s	B /m	S_0 /%	m /(plant·m^{-2})	State
Run-1	0.060	0.025	0.07	0.03	0.4	1	1	0.1	134	Submerged
Run-2	0.135	0.033	0.08	0.03	0.3	1	1	0.1	134	Emergent

This figure indicates that the average relative errors of the measured and predicted average flow velocity values in the cases Run-1, Run-2 are 3.24%, 3.36%, respectively. This finding indicates that the calculation method proposed in this paper fits well with the measured data and the errors are all within a reasonable range. The average sectional flow velocities for each zone calculated from Eqs. (17), (18) and (19) can be directly applied to the calculation of the dispersion coefficients.

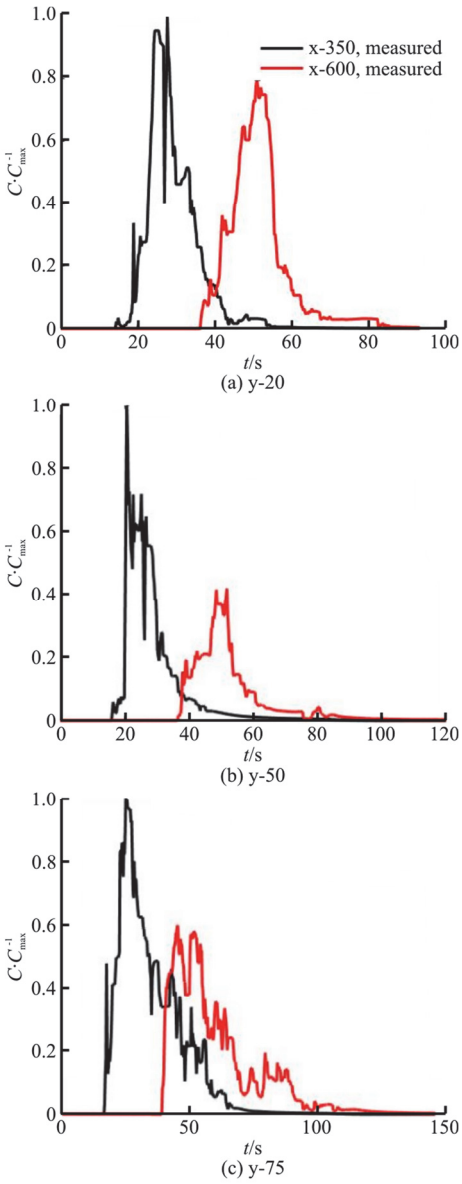

Fig. 5 (Color online) Pollutant concentration process in the case Run-1

3.2 *Pollutant concentration process*

Based on the measured data, the C-t curves are plotted for the pollutant concentrations in the cases Run-1, Run-2, as a function of the time using the peak concentrations in the pollutant concentration of each measurement line to nondimensionalize the upstream and downstream concentration values (Figs. 5, 6).

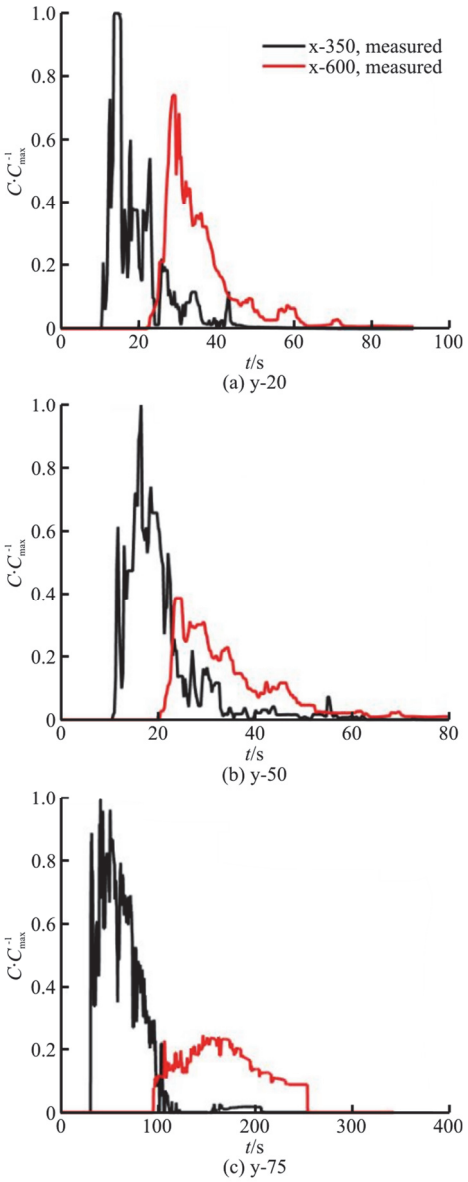

Fig. 6 (Color online) Pollutant concentration process in the case Run-2

In the upstream, the pollutants pass through the measurement points in a short period and the pollutants are concentrated, resulting in a small contaminant mass with a high concentration. Through the effect of the water movement, the pollutant flows through the downstream measurement point, demonstrating a wide range of low concentrations.

Figures 5, 6 show that the pollutant concentration processes at y-20 are similar for the cases Run-1, Run-2, which are mainly affected by the water movement, with high peak pollutant concentrations downstream. At y-50, the flow velocities in both cases Run-1, Run-2 are lower than those in the main

channel zone (y-20), so the peak pollutant concentrations downstream are lower relative to the main channel zone. The flow velocity in the floodplain zone is the smallest compared with the main channel and side slope zones. Thus, at y-75, the time and the concentration process of the pollutant concentrations in the cases Run-1, Run-2 in the downstream are the longest. In the floodplain zone, the submerged state of the vegetation, the flow rate, and the water depth conditions are different. Therefore, the flow rate in the case Run-1 is approximately 4.4 times higher than that in the case Run-2. At high flow velocities, the pollutants take the minimal time to pass through the upstream and downstream measurement points and vice versa. Simultaneously, in the floodplain zone in the case Run-1, the pollutants are rapidly diffused along the water flow direction due to the large flow velocity, resulting in a high peak concentration of the pollutants downstream. Meanwhile, in the floodplain zone in the case Run-2, the flow velocity is small and the pollutants slowly diffuse along the flow direction, resulting in a low peak concentration of the pollutants in the downstream.

3.3 *Dispersion coefficient validation*

The downstream predictions calculated from Eq. (25) are compared with the measured values to judge the degree of fit, and the K value in formula (25) is corrected on the basis this calculation.

$$R_t^2 = 1 - \left[\frac{\sum (M_t - P_t)^2}{\sum M_t^2} \right] \tag{26}$$

where M_t is the measured downstream concentration, P_t is the predicted downstream concentration.

As shown in Figs. 7, 8, the fitting degree of the measured and predicted pollutant values is better in the main channel zone (y-20) while that in the side slope zone (y-50) and the floodplain zone (y-75) is relatively poor. This finding is possibly due to the large flow velocity gradient in the side slope zone, which has a great effect on the dispersion of the pollutants, resulting in a relatively low accuracy of fit between the measured and predicted values.

In this experiment, the pollutant experiments are conducted in the main channel (y-20), the side slope (y-50), and the floodplain (y-75) zones, and the longitudinal dispersion coefficients are calculated by applying the "routing procedure" in each zone. The measured longitudinal dispersion coefficients of different zones are weighted and averaged in accordance with the area of each zone to obtain the longitudinal dispersion coefficient of the entire section, which is compared with that calculated by the two-zone model. The results are shown in Table 3.

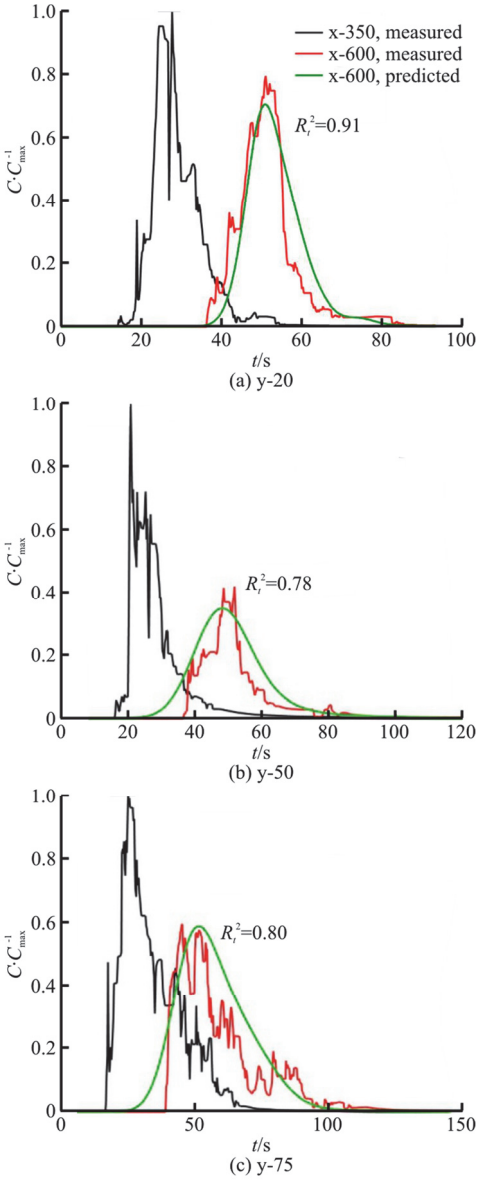

Fig. 7 (Color online) Measured and predicted pollutant concentrations in the case Run-1

Table 3 Measured and predicted values of the longitudinal dispersion coefficient (K_m is measured, K_p is predicted)

Run	K_m	K_{p1}	RE_1 /%	K_{p2}	RE_2 /%
Run-1	0.0067	0.0060	10.45	0.0064	4.48
Run-2	0.0208	0.0200	3.85	0.0216	3.85

Note: K_{p1} is calculated on the basis of the measured values of the average flow velocity of the section, K_{p1} is calculated on the basis of the predicted values of the average flow velocity of the section.

The measured and predicted values of the average flow velocity at the section are applied separately to the two-zone model, and the results are shown in

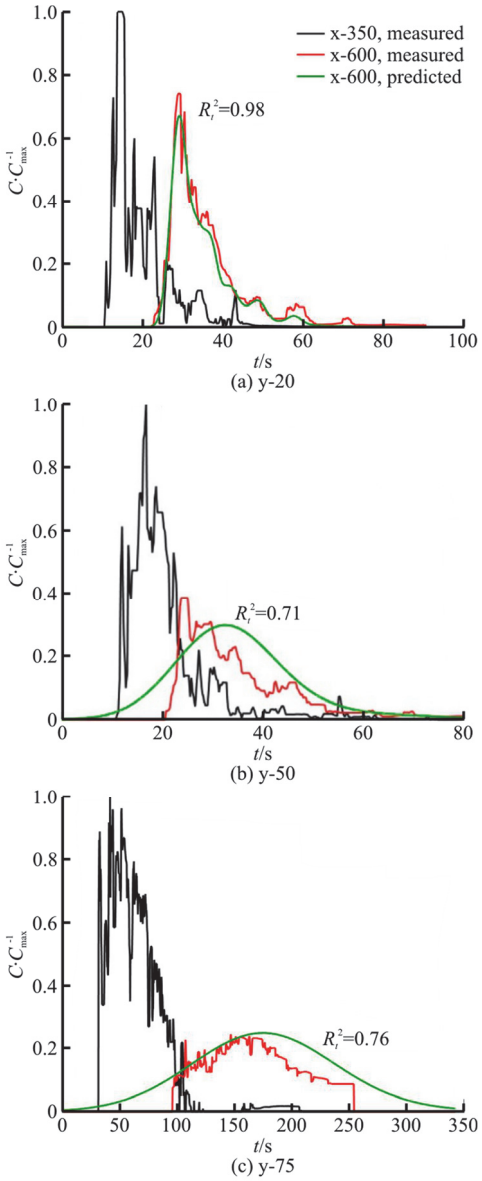

Fig. 8 (Color online) Measured and predicted pollutant concentrations in the case Run-2

Table 3. The average error of the longitudinal dispersion coefficient and the measured value of the longitudinal dispersion coefficient calculated on the basis of the average flow velocity value of the measured section is 7.15%, while that calculated on the basis of the predicted average velocity value of the section and the measured value of the longitudinal dispersion coefficient is 4.17%. Both values are within a reasonable range, and both errors are within reasonable limits. Therefore, the method of calculating the average section velocity and the two-zone model used in this paper are reasonable in predicting the dispersion coefficient of the floodplain vegetated compound channel.

3.4 *Comparison of dispersion coefficients*

Fischer, Deng, Zeng and Huai studied the non-vegetated floodplain and proposed the prediction formula for the longitudinal dispersion coefficient (Table 1). They also calculated the longitudinal dispersion coefficient of the entire flume, and the results are shown in Table 4.

Table 4 Predicted values of longitudinal dispersion coefficients calculated by different formulas

Run	K_m	$K_{p(\text{Fischer})}$	$K_{p(\text{Deng})}$	$K_{p(\text{Zeng and Huai})}$
Run-1	0.0067	0.0077	0.2040	0.3928
Run-2	0.0208	0.0336	0.8441	0.5968

Table 4 shows that the calculated results for Fischer, Deng, Zeng and Huai are all larger than the measured values, indicating that the presence of the vegetation changes the water movement characteristics of the river, hinders the transport of the pollutants, and substantially impacts the discrete process.

4. Conclusion

This paper studies the dispersion coefficient of a floodplain vegetated compound channel based on the transverse distribution of the longitudinal flow velocities through the flume experiments. The conclusions are as follows: (1) Based on the experimental design, this paper divides the compound channel into three sub-zones (the main channel, the side slope, and the floodplain) in the lateral direction. The lateral distribution of the longitudinal flow velocity in the floodplain-vegetated compound channel is obtained by solving for the coefficients from the analytical equation for each zone. The findings reveal that the model results are in good agreement with the experimental data. (2) Based on the analytical solution of the flow velocity distribution, this paper proposes a new method to calculate the average flow velocity of the section, and the calculation results can effectively simulate the measured average flow velocity data of the section. (3) The upstream and downstream pollutant concentrations are made dimensionless. Comparing the upstream and downstream pollutant concentration processes, the upstream and downstream pollutant clusters show small and large ranges with high and low concentrations, respectively. In the cases Run-1, Run-2, the pollutant concentration processes in the same area show similar characteristics. (4) Based on the predicted and measured average flow velocities of the section, this paper uses the two-zone model to predict the longitudinal dispersion coefficient and the average relative errors are 4.17%, 7.15%, indicating that the two-zone model can effectively predict the longitudinal dispersion coefficient. (5) Comparing the predicted equations for the longitudinal dispersion coefficients proposed by different

scholars, the predicted values are all larger than the measured values, indicating that the presence of the vegetation changes the water movement characteristics and substantially impacts the dispersion of the pollutants.

Acknowledgements

This work was supported by the Research project of China Three Gorges Corporation (Grant No. 202103399), the Talent Program of China Institute of Water Resources and Hydropower Research (Grant No. WE0199A052021) and the Basic Scientific Research Expense Project of IWHR (Grant No. WR0145B022021).

Compliance with Ethical Standards

Conflict of Interest: The authors declare that they have no conflict of interest.

Ethical approval: This article does not contain any studies with human participants or animals performed by any of the authors.

Informed consent: Informed consent was obtained from all individual participants included in the study.

References

[1] Liu C., Shan Y. Impact of an emergent model vegetation patch on flow adjustment and velocity [C]. *Proceedings of the Institution of Civil Engineers-Water Management*, 2022, 175: 55-66.

[2] Huai W. X., Li S., Katul G. G. et al. Flow dynamics and sediment transport in vegetated rivers: A review [J]. *Journal of Hydrodynamics*, 2021, 33(3): 400-420.

[3] Wang W. J., Huai W. X. Thompson S. et al. Steady nonuniform shallow flow within emergent vegetation [J]. *Water Resources Research*, 2015, 51(12): 10047-10064.

[4] Sun X., Shiono K. Flow resistance of one-line emergent vegetation along the floodplain edge of a compound open channel [J]. *Advances in Water Resources*, 2009, 32(3): 430-438.

[5] Huai W., Zhang J., Katul G. G. et al. The structure of turbulent flow through submerged flexible vegetation [J]. *Journal of Hydrodynamics*, 2019, 31(2): 274-292.

[6] Liu C., Shan Y., Sun W. et al. An open channel with an emergent vegetation patch: Predicting the longitudinal profiles of velocities based on exponential decay [J]. *Journal of Hydrology*, 2020, 582: 124429.

[7] Li Y., Wang Y., Anim D. O. et al. Flow characteristics in different densities of submerged flexible vegetation from an open-channel flume study of artificial plants [J]. *Geomorphology*, 2014, 204: 314-324.

[8] Fernandes J. N., Leal J. B., Cardoso A. H. Improvement of the lateral distribution method based on the mixing layer theory [J]. *Advances in Water Resources*, 2014, 69: 159-167.

[9] Wang W. J., Huai W. X., Li S. et al. Analytical solutions of velocity profile in flow through submerged vegetation with variable frontal width [J]. *Journal of Hydrology*, 2019, 578: 124088.

[10] Wu Z., Singh A., Foufoula-Georgiou E. et al. A velocity-variation-based formulation for bedload particle hops in rivers [J]. *Journal of Fluid Mechanics*, 2021, 912: A33

[11] Murphy E., Ghisalberti M., Nepf H. Model and laboratory study of dispersion in flows with submerged vegetation [J]. *Water Resources Research*, 2007, 43(5): 687-696.

[12] Huai W., Shi H., Song S. et al. A simplified method for estimating the longitudinal dispersion coefficient in ecological channels with vegetation [J]. *Ecological Indicators*, 2018, 92: 91-98.

[13] Liu X., Huai W., Wang Y. et al. Evaluation of a random displacement model for predicting longitudinal dispersion in flow through suspended canopies [J]. *Ecological Engineering*, 2018, 116: 133-142.

[14] Sonnenwald F., Stovin V., Guymer I. A stem spacing-based non-dimensional model for predicting longitudinal dispersion in low-density emergent vegetation [J]. *Acta Geophysica*, 2019, 67(3): 943-949.

[15] Shiono K., Knight D. W. Turbulent open-channel flows with variable depth across the channel [J]. *Journal of Fluid Mechanics*, 1991, 222: 617-646.

[16] Huai W., Xu Z., Yang Z. et al. Two dimensional analytical solution for a partially vegetated compound channel flow [J]. *Applied Mathematics and Mechanics (Engilsh Edition)*, 2008, 29(8): 1077-1084.

[17] Stone B. M., Shen H. T. Hydraulic resistance of flow in channels with cylindrical roughness [J]. *Journal of Hydraulic Engineering, ASCE*, 2002, 128(5): 500-506.

[18] Schlichting H., Gersten K. Boundary-layer theory [M]. NewYork, USA: McGraw-Hill, 1979.

[19] Pasche E., Rouvé G. Overbank flow with vegetatively roughened flood plains [J]. *Journal of Hydraulic Engineering,ASCE*, 1985, 111(9):1262-1278.

[20] Fischer H. B. "Discussion of 'simple method for predicting dispersion in streams' by McQuivey R S and TN Keefer T" [J]. *Journal of the Environmental Engineering Division*, 1975, 101(3): 453-455.

[21] Deng Z. Q., Singh V. P., Bengtsson L. Longitudinal dispersion coefficient in straight rivers [J]. *Journal of Hydraulic Engineering, ASCE*, 2001, 127(11): 919-927.

[22] Zeng Y., Huai W. Estimation of longitudinal dispersion coefficient in rivers [J]. *Journal of Hydro-Environment Research*, 2014, 8(1): 2-8.

[23] Wang Y., Huai W. Estimating the longitudinal dispersion coefficient in straight natural rivers [J]. *Journal of Hydraulic Engineering, ASCE*, 2016, 142(11): 04016048.

[24] Boxall J. B., Guymer I. Longitudinal mixing in meandering channels: New experimental data set and verification of a predictive technique [J]. *Water Research*, 2007, 41(2): 341-354.

[25] White B. L., Nepf H. A vortex-based model of velocity and shear stress in a partially vegetated shallow channel [J]. *Water Resources Research*, 2008, 44: W01412.

[26] Nepf H. M. Vegetated flow dynamics [J]. *The Ecogeomorphology of Tidal Marshes*, 2004, 59: 137-163.

[27] Nepf H. Drag, turbulence, and diffusion in flow through emergent vegetation [J]. *Water Resources Research*, 1999, 35(2): 479-489.

[28] Fischer H. B. Dispersion predictions in natural streams [J]. *Journal of the Sanitary Engineering Division*, 1968, 94: 927-943.

[29] Rominger J. T., Nepf H. Flow adjustment and interior flow associated with a rectangular porous obstruction [J]. *Journal of Fluid Mechanics*, 2011, 680: 636-659.

[30] Liu C., Nepf H. Sediment deposition within and around a finite patch of model vegetation over a range of channel velocity [J]. *Water Resources Research*, 2016, 51: 600-612.